The Size and Internal Structure of a Heterochromatic Block Determine Its Ability to Induce Position Effect Variegation in *Drosophila melanogaster*

Eugene V. Tolchkov,* Vanya I. Rasheva,* Silvia Bonaccorsi,† Thomas Westphal* and Vladimir A. Gvozdev*

**Department of Molecular Genetics of Animals, Institute of Molecular Genetics, Russian Academy of Sciences, Moscow 123182, Russia and †Centro di Genetica Evoluzionistica del CNR, Universitá di Roma "La Sapienza," Rome, Italy I-00185*

Manuscript received July 2, 1999
Accepted for publication November 24, 1999

ABSTRACT

In the *In(1LR)pn2a* rearrangement, the 1A-2E euchromatic segment is transposed to the vicinity of *X* heterochromatin (*Xh*), resulting in position effect variegation (PEV) of the genes in the 2BE region. Practically the whole *X*-linked heterochromatin is situated adjacent to variegated euchromatic genes. Secondary rearrangements showing weakening or reversion of PEV were obtained by irradiation of the *In(1LR)pn2a*. These rearrangements demonstrate a positive correlation between the strength of PEV of the *wapl* locus and the sizes of the adjacent heterochromatic blocks carrying the centromere. The smallest PEV-inducing fragment consists of a block corresponding to ~10% of *Xh* and containing the entire *XR*, the centromere, and a very proximal portion of *XL* heterochromatin. Heterochromatic blocks retaining the entire *XR* near the 2E region, but lacking the centromere, show no PEV. Reversion of PEV was also observed as a result of an internal rearrangement of the *Xh* blocks where the centromere is moved away from the eu-heterochromatin boundary but the amount of *X* heterochromatin remaining adjacent to 2E is unchanged. We propose a primary role of the *X* pericentromeric region in PEV induction and an enhancing effect of the other blocks, positively correlated with their size.

CHROMOSOMAL rearrangements that juxtapose euchromatin and heterochromatin induce a mosaic inactivation of euchromatic genes known as position effect variegation (PEV; see for reviews Henikoff 1990; Lohe and Hilliker 1995; Weiler and Wakimoto 1995; Zhimulev 1998). Recently, a number of euchromatic genes acting as enhancers or suppressors of PEV have been molecularly characterized and have been shown to encode for chromosomal proteins (Grigliatti 1991; Reuter and Spierer 1992; Lohe and Hilliker 1995; Jenuwein *et al.* 1998). By contrast, the molecular nature of PEV-inducing heterochromatic blocks is still largely unknown. Analysis of secondary rearrangements resulting in reversion of PEV indicates that remnants of heterochromatin in the regions of eu-heterochromatic junctions may be insufficient to maintain inactivation (Tartof *et al.* 1984; Pokholkova *et al.* 1993; Makunin *et al.* 1995; Tolchkov *et al.* 1997).

Early studies indicated that the strength of PEV correlates positively with the size of the heterochromatic block relocated near euchromatin (Panshin 1938). However, recent studies demonstrated that the strength of PEV of *white* does not correlate with the amount of heterochromatin adjacent to this gene (Howe *et al.* 1995).

The different ability of different heterochromatic blocks to cause PEV has been widely discussed (Spofford 1976). An important role of centromeric regions was proposed in the studies of PEV of heterochromatic genes removed from their heterochromatic location (Hilliker and Sharp 1988) but this hypothesis was later abandoned (Eberl *et al.* 1993; Weiler and Wakimoto 1995). Recently, it has been shown that the strength of PEV may depend not only on the size of the heterochromatic blocks adjacent to the euchromatic genes, but also on the distance of the eu-heterochromatic junction from the main heterochromatic block (Talbert *et al.* 1994; Henikoff *et al.* 1995; Henikoff 1997). It was proposed that failure of this junction to coalesce with the chromocenter may help the gene to escape inactivation (Henikoff *et al.* 1995). A similar hypothesis was put forward in the case of the inactivation of heterochromatic genes due to their transposition into a euchromatic environment (Wakimoto and Hearn 1990; Eberl *et al.* 1993).

Here we study a set of related rearrangements causing different extents of PEV of the genes located in the 2BE region. We have examined the effect on PEV not only of a stepwise decrease in the size of the *cis*-acting *X*-linked heterochromatic blocks, but also of their internal structure and their distance from the chromocenter.

MATERIALS AND METHODS

Fly stocks and crosses: The pericentric inversion *In(1LR)pn2a* (Figure 1A) and its derivatives are maintained over the *FM7* balancer, marked with $y^{31d}sc^{8}w^{a}v^{Of}$ *B* g^{4}. To evaluate

Corresponding author: Eugene Vladimirovich Tolchkov, Institute of Molecular Genetics, Kurchatov Sq. 2, Moscow 123182, Russia. E-mail: teugene@img.ras.ru

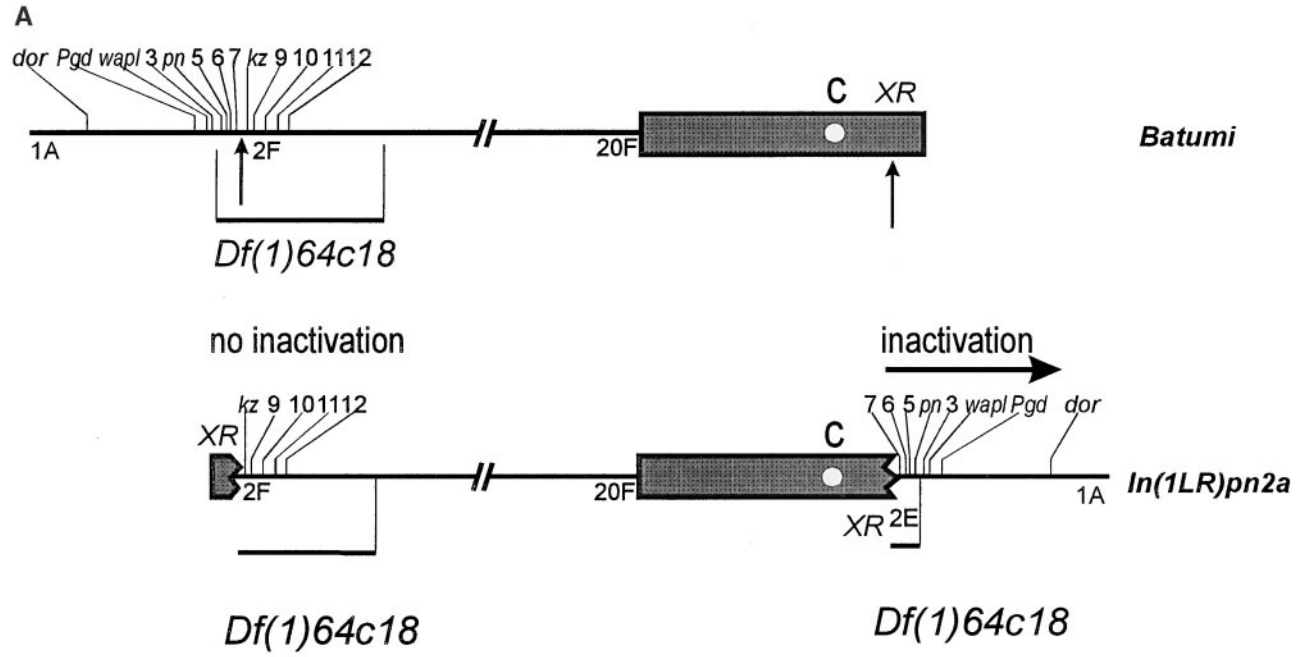

B

♀♀ *l74/Df(1)64c18* x ♂♂ *pn2a/B^{S}Y* (irradiated)

progeny:

inviable	viable when PEV is slight or lacking (inviable when PEV is strong)
♀♀ *pn2a/ l74*	♀♀ Rev(*pn2a*)/ *l74*
♀♀ *pn2a/Df(1)64c18*	♀♀ Rev(*pn2a*)/*Df(1)64c18*
♂♂ *l74/ B^{S}Y*	
♂♂ *Df(1)64c18/ B^{S}Y*	

C

♀♀ *l74·B^{S}Y/Df(1)64c18* x ♂♂ *pn2a/B^{S}Y* (irradiated)

progeny:

inviable	viable
♀♀ *pn2a/ l74*	♀♀ *pn2a/ l74·B^{S}Y* (extreme *wapl* phenotype)
♀♀ *pn2a/Df(1)64c18*	♀♀ Rev(*pn2a*)/ *l74·B^{S}Y*
♂♂ *l74/ B^{S}Y*	
♂♂ *Df(1)64c18/ B^{S}Y*	
♀♀ *pn2a/Df(1)64c18·B^{S}Y*	viable when PEV is slight or lacking (inviable when PEV is strong)
♂♂ *l74·B^{S}Y/B^{S}Y*	
♂♂ *Df(1)64c18·B^{S}Y/B^{S}Y*	
	♀♀ Rev(*pn2a*)/*Df(1)64c18·B^{S}Y*
	♀♀ Rev(*pn2a*)/ *l74*
	♀♀ Rev(*pn2a*)/*Df(1)64c18*

Figure 1.—Origin and structure of the *In(1LR)pn2a* rearrangement (A) and genetic systems for recovery of secondary rearrangements (B and C). (A) Diagrams representing the Batumi *X* chromosome (top) and the *In(1LR)pn2a* chromosome (bottom). Heterochromatin is depicted as a solid block; euchromatin is depicted as a thin line. Euchromatic boundaries are indicated according to the Bridges polytene map. The numbers above each diagram indicate vital loci in the region saturated by lethals (Gvozdev *et al.* 1975). *Pgd*, *wapl*, and *kz* correspond to vital loci 1, 2, and 8, respectively; *pn* corresponds to the nonvital locus 4. Vertical arrows indicate the breakpoints resulting in the *pn2a* rearrangement. The region uncovered by *Df(1)64c18* is also shown. C, centromere. *XR*, right arm of *X* chromosome. (B) Selective system for the recovery of secondary rearrangements. Rev, reversions. Irradiated *In(1LR)pn2a* / *B^{S}Y* males were crossed to *y l74 pn w^a ct v* / *y Df(1)64c18 pn w^a ct v* females. Viable Rev(*pn2a*) / *l74* and Rev(*pn2a*) / *Df(1)64c18* females were crossed to *FM7*, *y^{31d} sc^8 w^a v^{OF} B g^4* / *Y* males to balance putative revertant chromosome. Recessive markers were used to distinguish Rev(*pn2a*) from recombinant chromosomes in the progeny of Rev(*pn2a*) / *l74* or Rev(*pn2a*) / *Df(1)64c18* females. (C) Modified scheme of crosses to obtain secondary rearrangements using the *y l74 pn w^a ct v* · *B^{S}Y^L* chromosome.

the effect of the *Y* chromosome on *wapl* variegation in *pn2a* derivatives R/*FM7*, $y^{31d}sc^{8}w^{a}v^{Of}$ *B* g^{4} females (R, secondary rearrangements) were crossed to *y l(1)74 pn* w^{a} *ct v* · $B^{S}Y^{L}/w^{+}$ *Y* males where *l(1)74* is a lethal allele of the *wapl* gene (Gvozdev *et al.* 1975), hereafter referred to as *l74*. For details of mutants, balancers, and chromosome deficiencies, see Lindsley and Zimm (1992).

Selective system to obtain secondary rearrangements: Secondary rearrangements (R) were induced by irradiation (4 kR) of *pn2a*/$B^{S}Y$ males (Figure 1B). Irradiated males were crossed to *y l74 pn* w^{a} *ct v*/*y Df(1)64c18*w^{a}*ct v* females. Selection was based on the strong inactivation of several vital genes due to PEV in the *pn2a* chromosome. Suppression of PEV in secondary rearrangements restores gene activity and results in survival of the R/*l74* or R/*Df(1)64c18* females carrying the rearrangement. Selected females were crossed to *FM7*, $y^{31d}sc^{8}w$ $v^{Of}B$ $g^{4}Y$ males to balance the revertant chromosome. Recessive markers (w^{a}, *ct*, *v*) were introduced to distinguish R from a recombinant chromosome in the progeny of R/*l74* or R/*Df(1)64c18* females. Using this selective system, only rearrangements causing complete PEV loss were obtained.

To select rearrangements resulting in incomplete suppression of PEV, *Y* chromosome material was introduced into the system using the *l74* · $B^{S}Y^{L}$ chromosome (see above; Figure 1C). As a result, eclosed *pn2a*/*l74* · $B^{S}Y^{L}$ females survived, although most individuals showed an extreme *wapl* phenotype ("cut wings," angle between wings amounts to 180°; see below) and died before laying eggs. Selected females were balanced over *FM7* by crossing to *FM7*/*Y* males.

Estimation of PEV: *wapl* locus inactivation was tested in R/*l(1)74* females carrying a secondary rearrangement over a normal *X* chromosome. The following phenotypic traits were monitored: "wings apart"; cut wings (or excised); irregular rows of facets; and decrease of viability.

The penetrance of the cut wings phenotype was measured as percentage of wings with cuts among all individuals. The wings apart phenotype was quantitatively evaluated both by counting the percentage of flies with an enlarged angle between wings and by measuring the angle between wings. Angle was measured using a scaled plate, where micro-dials were graduated in 10°. Increase of angle value over 30° (experiment 1) or over 45° (experiment 2) was taken as an indication of a mutant *wapl* phenotype (see Table 2), as compared to the angle of 20–30° in wild-type flies. The "irregular facets" phenotype was measured as the mean percentage of eye surface with irregular ommatidial packing. A disturbance of faceting was taken into account starting with a detectable spot comprising 2–3% of eye surface (~10 irregularly arranged facets out of 400). The eye surface was arbitrarily divided into eight sectors, each encompassing ~12–13% of the surface. The ratio of mutant to the total eye surface was estimated using this unit of evaluation. The low level of variegation was estimated directly by counting the number of facets in the area of mutant tissue. Fortuitous faceting disturbance amounts barely to 0.03% of eye surface in Batumi-L and other wild-type stocks.

The inactivation of the *dor* locus was tested in R/dor^{l} females. PEV intensity of the *dor* gene was evaluated as the percentage of eyes with yellowish spots as well as by estimation of the yellow area of the eye surface.

Analysis of segregation between the *Y* chromosome and recombinants containing parts of different rearrangements: To analyze the segregation between the $y^{2}Y43T$ chromosome and the recombinant (Rec) $sc^{S1p}m141^{d}$ (see legend to Figure 4A) or $r16^{p}m141^{d}$ (see legend to Figure 4C) chromosomes, *C(1),dor*/*Dp(1)*$y^{2}Y43T$ females were crossed to Rec/*Dp(1)*$y^{2}Y43T$ males. Chromosome $y^{2}Y43T$ carries the 1A-2F duplication covering *dor*. Appearance of *dor* females in the progeny indicates the occurrence of *X-Y* nondisjunction in males.

Cytological analysis of polytene chromosomes: Fertile R/*Y* males (*r9*, *r30*, *r20*, *pn2a*, *m100*, and *m141*) and R/*FM7* females (males carrying *r4*, *r24*, *r16*, and *r35* were sterile or inviable) were crossed to *y ac sc w* females or males, respectively. Salivary glands were dissected from R/*y ac sc w* third instar female larvae with yellow malpighian tubules (w^{+} phenotype).

Mitotic chromosomes: Preparation and sequential staining of mitotic chromosomes with Quinacrine, Hoechst, and N-banding were carried out as described (Gatti *et al.* 1994).

RESULTS

Recovery of secondary rearrangements: The *In(1LR) pn2a* original rearrangement (hereafter referred to as *pn2a*; Ilyina *et al.* 1980; Tolchkov *et al.* 1984) has a euchromatic breakpoint in 2E, which disrupts the *Vinculin* gene (Alatortsev *et al.* 1997), and a heterochromatic breakpoint in the right arm of the *X* chromosome (Tolchkov *et al.* 1997; Figure 1A). As a consequence, the 1A-2E segment, encompassing seven identified loci (including *pn*, *wapl*, and *Pgd*; Gvozdev *et al.* 1975), is transposed adjacent to the centric heterochromatic block. These genes exhibit strong PEV (Alatortsev *et al.* 1982; Tolchkov *et al.* 1984, 1997). Inactivation spreads far from the breakpoint, affecting the *dor* locus situated ~700 kb apart from heterochromatin; *kz* and four additional loci adjacent to *XR* telomere in *pn2a* show no PEV (Figure 1A). Inactivation of euchromatic genes in the *pn2a* inversion resulted in inviability of *pn2a*/*l74* as well as *pn2a*/*Df(1)64c18* females (Figure 1B). *l74* is a lethal allele of the *wapl* gene and *Df(1)64c18* uncovers *pn* and several vital loci designated as complementation groups 5, 6, and 7 (Figure 1A).

Selection of *pn2a* secondary rearrangements with a decrease or complete loss of PEV was based on the restoration of activity of several vital genes affected by PEV in the *pn2a* chromosome. Two different cross schemes have been used to select secondary rearrangements with complete (Figure 1B) and partial (Figure 1C) reversion of PEV. Using the first scheme of selection, 4 secondary rearrangements were obtained (Figure 1B), while 18 secondary rearrangements were selected using a modified scheme of screening (Figure 1C). In a set of secondary rearrangements, the correlation between the decrease of PEV and the sizes and structures of *cis*-acting heterochromatic blocks was studied.

The structures of rearrangements were defined by mitotic chromosome staining as well as by genetic and polytene chromosome analysis. The centromere region (h33) and the eu-heterochromatic boundary (2E-h34) were identified by Quinacrine staining and N-banding, respectively. Centromere position was determined by genetic tests when the Quinacrine region was split. The nucleolus organizer region (NO) h29 is detected as a constriction, and the other *Xh* segments are identified by their peculiar fluorescence patterns after Hoechst staining. These results are summarized in Figure 2

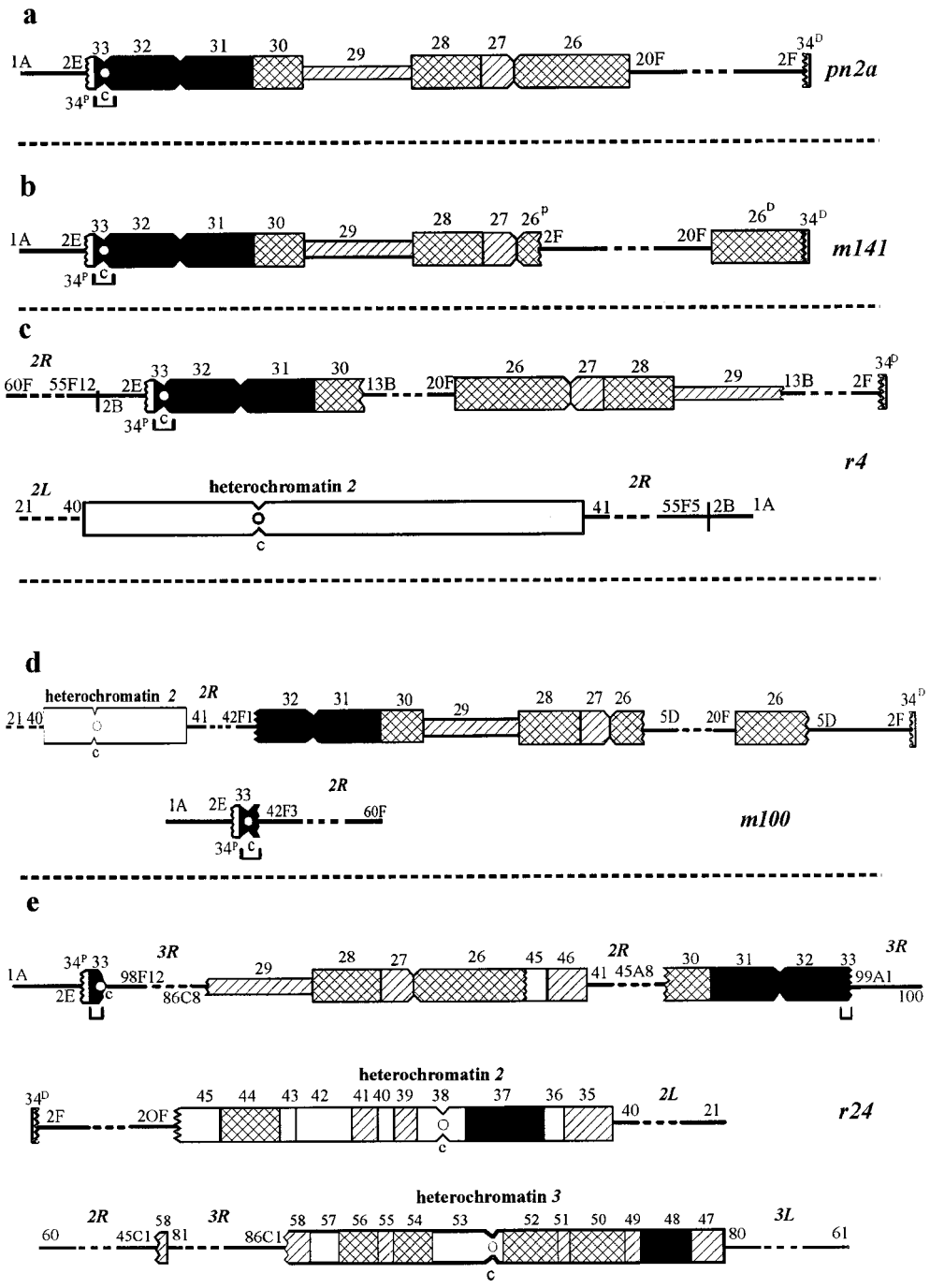

Figure 2.—Diagramatic representation of rearrangements after Hoechst 33258 staining. Heterochromatic segments are indicated according to Gatti *et al.* (1994); euchromatin is depicted as a thin line. Solid segments indicate bright fluorescence; cross-hatched segments indicate moderate fluorescence; hatched segments indicate dull fluorescence; and open segments indicate no fluorescence. The horizontal bracket indicates the pericentromeric Quinacrine-fluorescent region (h33). The h34 segment is differentiated by N-banding. C, centromere.

(schemes of rearrangements) and Figure 3 (mitotic chromosomes).

On the basis of the structure of the heterochromatic block juxtaposed to 2E (see below), the rearrangements can be grouped into three classes.

Rearrangements with decreasing amounts of the *cis*-acting heterochromatic block (class 1): *m141* is an inversion with a euchromatic breakpoint in 2F and a heterochromatic breakpoint in h26 that separates the distal portion of h26 from the main block of *Xh* (Figures 2b and 3b). Detection of free recombination with *In(1)sc*^{S1} and recovery of males carrying the 1AB deletion (Figure 4A) demonstrate the presence of the 2F-20F inversion. The presence of the 1AB deletion was inferred from the recovery of the *yellow*^{2} males carrying a recombinant chromosome and the *y*^{2}*Y43T* duplication (Figure 4A). The observed high frequency of nondisjunction of sex chromosomes in these males was attributed to a deletion of NO in the recombinant chromosome, taking into account the role of NO region in sex chromosome disjunction (McKee 1996).

r4 is a complex rearrangement that splits the *Xh* block into a proximal part (h30-h34^{P}) that remains adjacent to 2E and a distal part (h26-h29) that is separated from

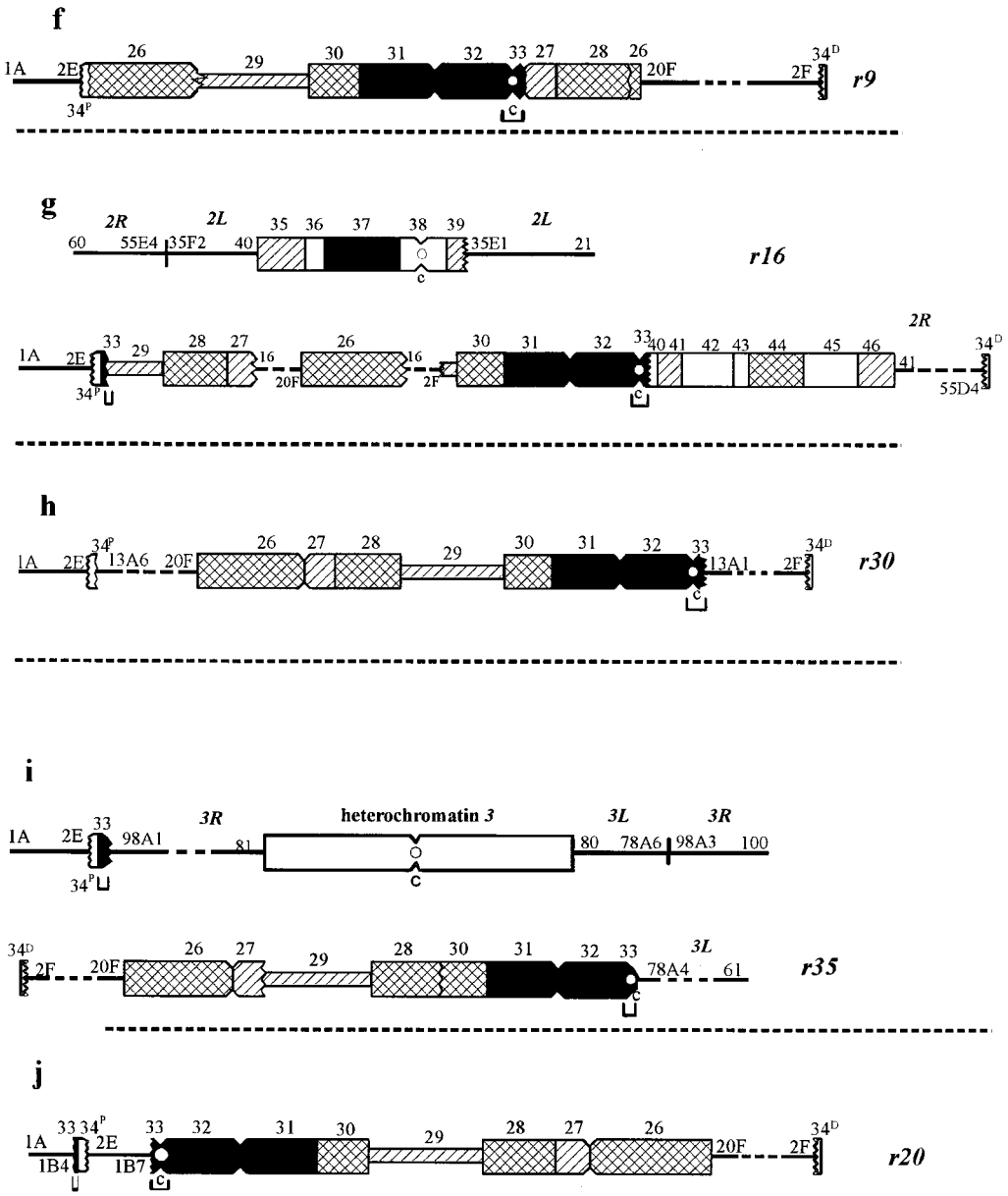

Figure 2.—*Continued.*

the centric segment by the 13B-20F euchromatic fragment (Figures 2C and 3C). Polytene chromosome analysis revealed also the presence of a translocation, T(1;2)2A;55F5-12, which in mitotic figures results in an increased length of the euchromatic fragment attached to the proximal *Xh* block (Figure 3C).

m100 is a translocation, *T(1;2)*h32/h33;42F1-3, that results in a small acrocentric chromosome, carrying the N-banded h34^{p} region and the whole Quinacrine-stained block (h33) attached to the euchromatic 1A-2E region (Figures 2d and 3d). The rest of the *Xh* block is transposed to *2R* and is split into two fragments by an additional inversion, *In(1)*5D;h26 (Figures 2d and 3d).

r24 is a complex translocation involving chromosomes *X*, *2*, and *3*. In mitotic chromosome preparations the *X*-linked Quinacrine-bright material appears split into two equal parts, located at the opposite ends of a chromosome containing two *Xh* blocks separated by a euchromatic segment (Figure 3e). Polytene chromosome analysis allowed us to show that this euchromatic segment comprises both chromosome *2* and *3* bands (Figure 2e). Moreover, genetic analysis (see Figure 4B) confirmed that the *X* centromere is located near the 2E euchromatic region in this rearrangement.

Internal rearrangements that relocate distal *Xh* adjacent to acentric *XR* material (class 2): *r9* is a secondary rearrangement of the h26-h33 region. The h26 region is flanked by the NO constriction (h29) and the N-banded h34^{p} region, while the Quinacrine (Q)-bright band is located adjacent to the dull fluorescent segment h27-h28 (Figures 2f and 3f). Analysis of NO-mediated recombination between *r9* and the *Y* chromosome corroborates the presented structure (data not shown).

r16 is a complex rearrangement, *Tp(1;1)*h33;h29;2F+

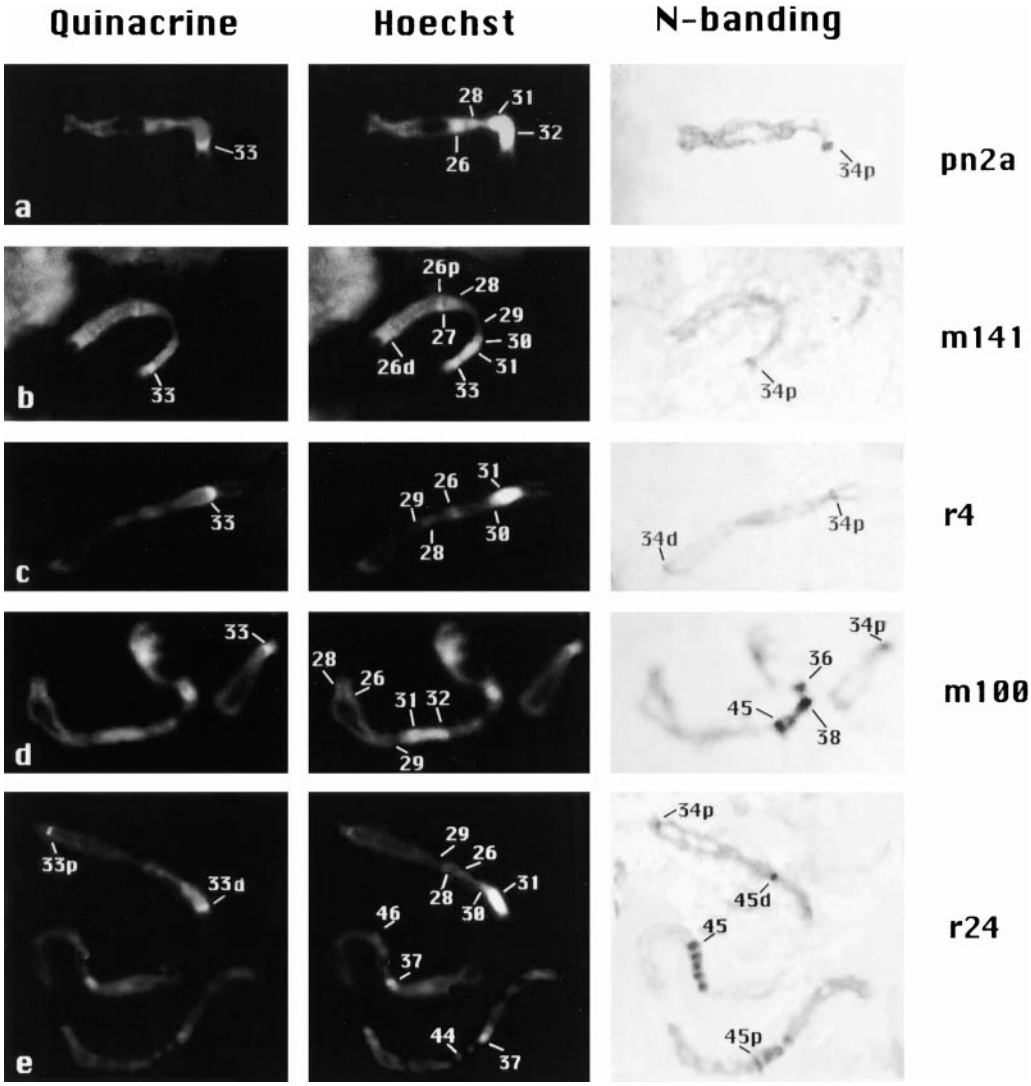

Figure 3.—Cytological characterization of rearrangements by sequential Quinacrine staining, Hoechst staining, and N-banding. The numbers identify the heterochromatic regions (*cf.* with Figure 2 and Gatti *et al.* 1994). p and d indicate the proximal and distal portions of a broken region, respectively. In e note the reduced h45 N-band present on the second chromosome involved in the r24 rearrangement (45p), as compared to a normal-sequence second chromosome (45).

In(1)16;h26/h27 + *T(1;2)*, resulting in a marked decrease of the heterochromatic mass adjacent to the 2E region (Figure 2g). The transposed centric block comprises most (75–80%) of the *X*-linked Q-bright material, the rest of which is detected near h34^{p} (Figure 3g). Recovery of the *r16^{p}m141^{d}* recombinant chromosome carrying no small block of Q-bright material (data not shown) allowed us to map the centromere within the major Q-stained band (Figure 4C). NO appears to be located near the tiny Q-band and h34^{p} (Figure 3g), but genetic analysis indicated that a piece of NO must be left adjacent to the h30 region (Figure 4C).

Rearrangements that separate the acentric *XR* region from the main heterochromatic block (class 3): Here the structures of three representative rearrangements are presented:

r30 is a previously described (Tolchkov *et al.* 1997) inversion whose structure is diagramatically reported in Figure 2h.

r35 is a complex rearrangement involving chromosome *3* (Figure 2i). The 1A-2E region is translocated to the rearranged third chromosome together with an adjacent *Xh* segment consisting of region h34^{p} and an acentric fragment of the Q-bright h33 region (Figures 2i and 3i). The structure of the main *Xh* block associated with *3L* is also modified by an additional inversion involving regions h28 and h29 (Figures 2i and 3i).

r20 is a secondary inversion with a heterochromatic breakpoint in the distal portion of h33 and a euchromatic breakpoint in region 1B. As a result, a small heterochromatic segment comprising h34^{p} and h33^{d} is separated from the main *Xh* block containing the centromere by the 2E-1B euchromatic region (Figures 2j and 3j).

A total of 13 rearrangements leading to full suppression of PEV carry a putative heterochromatic breakpoint near the 2E-heterochromatin boundary and represent translocations of acentric 1A-2E region to distal euchromatin of autosomes (10 rearrangements) or *X* chromo-

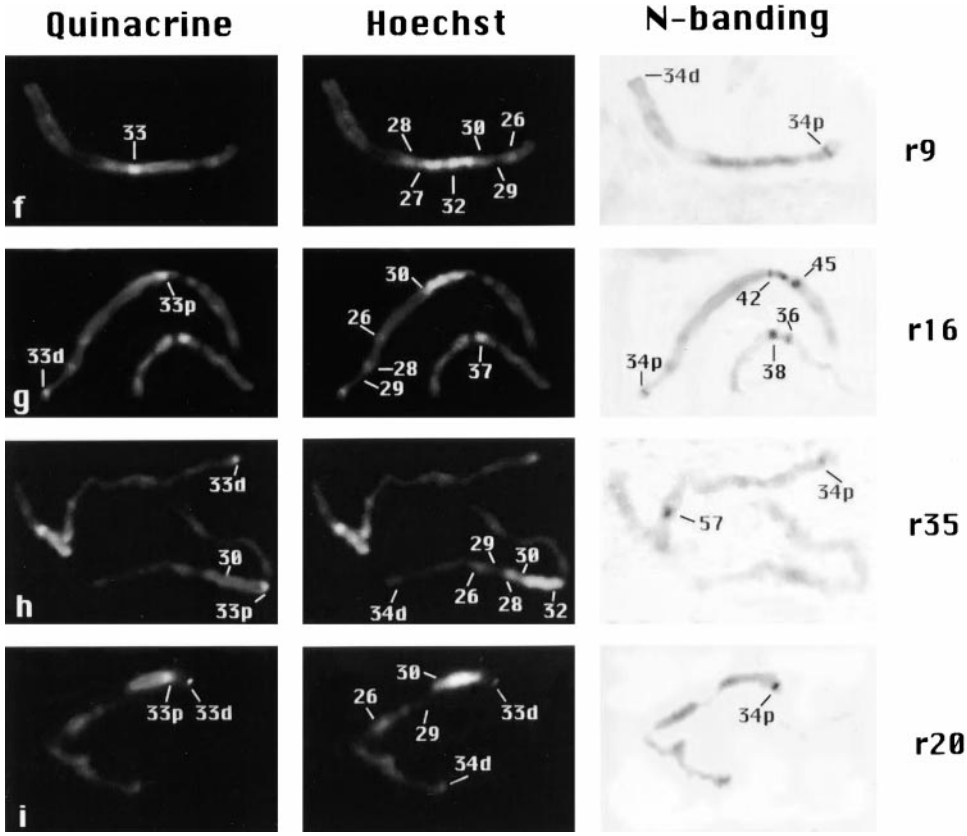

Figure 3.—*Continued.*

somal inversions (3 rearrangements). These rearrangements were characterized by polytene chromosome analysis and represent the most numerous group of rearrangements.

PEV of the *wapl* locus in secondary rearrangements: The strength of PEV exerted by the various rearrangements was tested by studying the degree of *wapl* locus inactivation in R/*l74* female progeny from crosses ♀♀R/*FM7* × ♂♂*l74*/w^+Y (see materials and methods). The following phenotypic traits were detected: wings apart, cut wings (or excised), and irregular ommatidial packing. Decrease of viability was also evaluated.

In experiment 1, stocks carrying a nonmarked *Y* chromosome were used (except the *r24* stock, carrying a B^SY chromosome). However, in some rearrangements a high level of *X* chromosome nondisjunction was observed (Table 1), resulting in females carrying a *Y* chromosome, a well-known suppressor of PEV. To avoid artifacts in measuring PEV, all the stocks used for experiment 2 carried a B^SY chromosome. The percentage of eye surface with irregular faceting in R/*l74*·B^SY^L females could not be estimated due to effects of the B^S marker (Bar eyes). However, correlation of the strength of irregular faceting with the wing phenotypes indicates that faceting is also affected by PEV. In Table 2 the rearrangements are reported in order of decreasing strength of PEV. As can be seen, the introduction of a *Y* chromosome decreases *wapl* inactivation in all cases.

A stepwise reduction of the heterochromatic block adjacent to the 2E region (class 1 rearrangements) causes a gradual decrease of PEV: All four rearrangements (*m141*, *r4*, *m100*, and *r24*) belonging to class 1 exhibit a positive correlation between the size of the heterochromatic block remaining adjacent to 2E and the extent of *wapl* inactivation.

As can be seen in Table 2, viability is affected only by the secondary inversion *m141*, which, however, exhibits a significant increase of viability as compared to the original rearrangement *pn2a*. In both cases, addition of a *Y* chromosome fully restores viability (Table 2, experiment 1).

Judging from the penetrance of the cut wings phenotype (percentage of wings with cuts among total scored flies), the extent of *wapl* inactivation diminishes gradually in the four rearrangements belonging to class 1 (*m141*, *r4*, *m100*, and *r24*). The percentage of cut wings drops from 94% in *m141*/*l74* females to 35% in *r24*/*l74* females (experiment 1). These results were confirmed in experiment 2, although a comparison of *r4*/*l74* with *m100*/*l74* females revealed no significant difference in the number of cut wings. The number of cut wings drastically diminished after addition of a *Y* chromosome (experiment 1). Experiment 1 also demonstrates a significant decrease in the number of cut wings among the flies bearing the *m141* rearrangement as compared to the individuals with *pn2a* inversion.

The decrease of PEV in *m141* was confirmed when the penetrance of the wings apart phenotype was evaluated

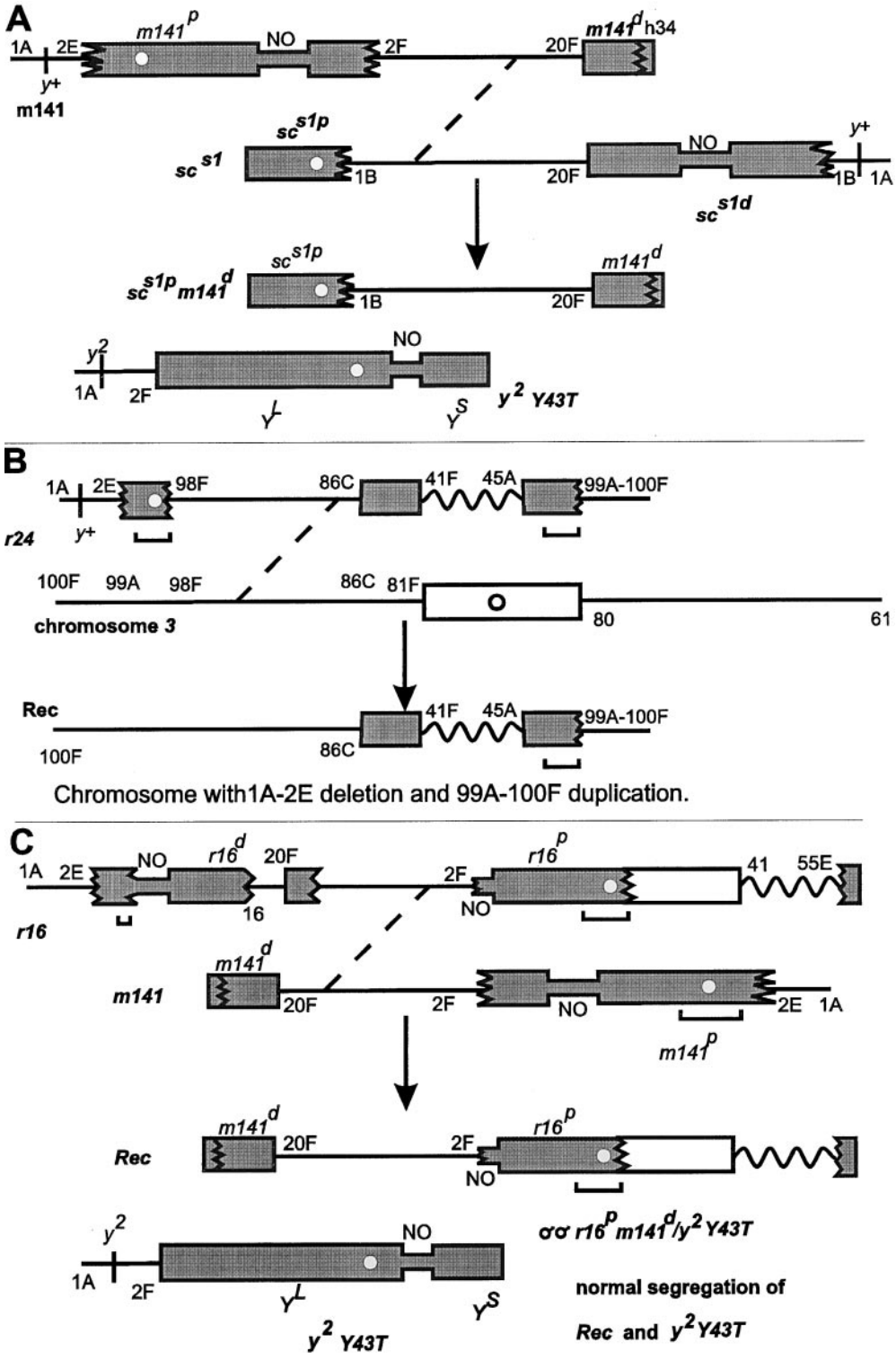

Figure 4.—Genetic analysis of rearranged chromosomes. Open circles indicate the centromere. Recombination events are indicated by dashed oblique lines. Cytological localization is according to the Bridges map. Other designations are as in Figure 2. (A) Recombination between *m141* and *In(1)sc*^{S1}. The recombinant transmittable chromosome *sc*^{S1p}*m141*^{d} carries no NO (see text for further details). The *y*^{2}*Y43T* chromosome carries a 1A-2F duplication covering the 1AB deficiency in the recombinant chromosome. (B) Mapping of the centromere near the 2E region in the *r24* rearrangement involving chromosomes *1*, *2*, and *3* (see Figure 2e). The wavy line represents euchromatin of chromosome *2*. We infer that the centromere is not contained in the Q-bright material transposed to the 99A region because we failed to recover the putative recombinant chromosome Rec (bottom) lacking the 1A-2E region. The deletion of the 1A-2E region may be detected by a recovery of *y*^{2} males in a progeny of cross[♀♀*r24*/*FM7* × ♂♂*Df(1)pn2a·B*^{S}*Y*^{L}/*y*^{2}*Y43T*]. No *y*^{2} males were detected among 369 *y*$^{+}$ males (genotype *r24*/*y*^{2}*Y43T*) and 236 *FM7*/*y*^{2}*Y43T* males, although ~20 *y*^{2} [*Df(1)1A-2E*/*y*^{2}*Y43Y*] recombinant males may be recovered as a result of homologous recombination in the 86C-98F region (10 cM). Interchromosomal effect of *FM7* balancer may compensate for the decrease of recombination because of rearrangement. The absence of *y*^{2} males indicates that putative recombinant chromosome Rec is acentric. (C) Centromere and NO mapping in the *r16* rearrangement. Heterochromatin of chromosome *1* is shaded. Recombination between *r16* and *m141* (see Figure 2, b and g) leads to a recombinant chromosome lacking the 1A-2E region. The observed normal segregation of centric recombinant and *y*^{2}*Y43T* chromosomes can be explained by the presence of NO fragment adjacent to the 2F euchromatic region, taking into account the role of rDNA in segregation of *X* and *Y* chromosomes (McKee 1996). Thus, a heterochromatic break of the *r16* rearrangement must have occurred within the NO region, splitting it into two unequal parts (Figure 2g).

(Table 2). A further decrease in the number of wings apart flies was observed for the *r4* and *r24* rearrangements while the estimation of the mean angle between wings demonstrated the strong decrease of *wapl* inactivation occurring in *r24* as compared to *m100*.

Evaluation of the expression of the irregular facets

TABLE 1

Traits of stocks with rearrangements (R)

R	R/*Y* males		Females	
	Viability	Fertility	Viability of R/R females	Segregation of *X* chromosomes in R/*FM7* females
pn2a	30–50%	N	+	N
r4	0[a]	nt	nt	N
r9	N	N	+	N
r16	N	~1%	0	N
r20	N	N	+	N
r24	N	0	nt	D[b]
r30	N	N	+	N
r35	N	0[c]	0	D
m100	N	N	+[d]	D
m141	<1%	N	0	N

N, normal viability and fertility of males; normal segregation of *X* chromosomes in females. +, viable R/R females. 0, inviability or infertility. nt, not tested. D, segregation of *X* chromosome in R/*FM7* is drastically disturbed.

[a] Viable in combination with suppressors of variegation.

[b] Twofold reduced fertility.

[c] Low fertility (~10% of normal), reduced to zero after several years.

[d] Extremely low.

phenotype confirmed the progressive decrease of PEV in these secondary rearrangements, from *m141* to *r4*.

Thus, a careful estimation of the pleiotropic effects of *wapl* inactivation allows us to conclude that the extent of variegation is correlated with the quantity of adjacent *X*-linked heterochromatin. We detected a gradual decrease of *wapl* variegation for four rearrangements (*m141*, *r4*, *m100*, and *r24*), where the heterochromatic block remaining adjacent to 2E was stepwise reduced. A pronounced *wapl* variegation is detected even in the *r24* rearrangement carrying barely 10% of the whole *Xh* block, comprising approximately half of the Quinacrine-positive band h33, the centromere, and the N-banded region h34 (Table 2; Figure 2e). Elimination of the heterochromatic segments h26-h27 distal to the NO region (h29) resulted in a noticeable decrease of variegation strength. Thus, practically the whole *Xh* region appears to contribute to the strength of PEV.

Internal rearrangements in the *Xh* block (class 2) suppress PEV: The extent of PEV was shown to be decreased drastically in *r9* or even eliminated in *r16*, although the whole (*r9*) or a significant part (*r16*) of the *Xh* block remained adjacent to 2E in these two rearrangements (Figure 2, f and g). In the *r9* rearrangement, an internal inversion of most of the *Xh* block, determining a separation of the centromere region from the eu-heterochromatic boundary, results in a drastic weakening of *wapl* variegation (Figure 2f; Table 2). In fact, inactivation of the *wapl* gene was detected only by disturbance of ommatidial packing affecting small areas of eye (from fractures of a single row of facets up to 5% of altered faceting, with a 2% mean value of mutant eye surface). No *wapl* wing phenotype was observed in *r9*/*wapl* females. To detect *wapl* inactivation distinctly, *r9*/*wapl* females were produced by reciprocal cross (*l74*/*FM7* × *r9*/*Y*), taking into account the known paternal effect resulting in enhanced variegation (Spofford 1976). Of these *r9*/*l74* females, 4% exhibited cut wings.

No *wapl* variegation was observed in *r16*, where the *Xh* block juxtaposed to 2E is rearranged and lacks the centromere (Figure 2g). However, the amount of heterochromatic material that remains near 2E in *r16* is larger than in *r24*, a secondary rearrangement that causes strong variegation. These results indicate that the strength of PEV may be determined by the specific arrangement of the *X* heterochromatic segments.

Small acentric pieces of *XR* juxtaposed to the 2E region (class 3 rearrangements) do not induce variegation: Most of the secondary rearrangements belonging to class 3 have no centromere in the *XR* heterochromatic block that remains juxtaposed to 2E and cause no variegation. In these rearrangements centromere is separated from the *XR* portions by eight or more sections of the Bridges map. In particular, no variegation of the *wapl* gene was detected in *r30* (Tolchkov *et al.* 1997) as well as in *r35*, where the 2E region is associated with the h34 and h34-h33 material, respectively (Figure 2, h and i). The *r20* rearrangement (Figure 2j) is an exception in that it causes a variegation of the *wapl* gene that is stronger than in *r24* (Table 2). A possible explanation of this unexpected result will be provided in the next section.

Peculiarities of the *r20* rearrangement: Several observations exclude the possibility that in *r20* inactivation

TABLE 2

Variegation of the *wapl* locus

Class of R	Size of heterochromatic block	Viability			% of cut wings			% of females with enlarged angle between wings (wings apart)[b]			Mean angle between wings[c]	% of eye surface with disturbed faceting
		Experiment 1		Experiment 2	Experiment 1		Experiment 2	Experiment 1		Experiment 2	Experiment 2	Experiment 2
		R/*l74*	R/*l74*·Y	R/*l74*	R/*l74*	R/*l74*·Y	R/*l74*	R/*l74*	R/*l74*·Y	R/*l74*	R/*l74*	R/*l74*
pn2a	h34-h26	nt	106 (210/198)	0[a] (0/108) ***	nt	56 (235/416) ***	—	nt	75 (157/210) *	—	—	—[a]
m141 1	h34-h27	29 (50/173)	113 (132/117)	18 (24/131)	94 (73/78) **	43 (112/262)	100 (48/48) ***	80 (40/50)	52 (68/132) ***	100 (24/24)	131 ± 29.0	77 ± 12.2 (45) **
r4 1	h34-h30	84 (118/140)	114 (158/137)	116 (74/64)	79 (150/190)	15 (46/312)	85 (115/136)	83 (98/118)	8 (12/158)	96 (64/67)	107 ± 5.0	37 ± 2.7 (138) **
m100 1	h34-h33	nt	nt	87 (42/48)	nt ***	nt ***	75 (63/84) *	nt	nt	86 (36/42) **	94 ± 7.2 ***	25 ± 2.9 (84)
r20 3	h34-part of h33	125 (56/44)	103 (112/109)	106 (100/94)	49 (51/104) *	2 (4/224)	63 (127/202) ***	71 (40/56)	0 (0/112)	62 (63/101) ***	57 ± 3.6 ***	22 ± 1.7 (202) **
r24 1	h34-part of h33	86 (57/65)	69 (20/29)	102 (55/54)	35 (39/112) ***	0 (0/40)	20 (22/110) ***	47 (27/57)	0 (0/20)	13 (7/55)	30 ± 1.9	7 ± 1.1 (110)
r9 2	h34-h26	104 (206/199)	88 (195/222)	nt	0 (0/410)	0 (0/390)	0 (0/402)	0 (0/206)	0 (0/195)	0 (0/201)	25[c]	2 ± 0.3 (402)

R, rearrangement. Variegation traits are evaluated for the R/*l74* or R/*l74*·Y females as compared to FM7/*l74* sisters. Severe nondisjunction of *X* chromosomes was detected in crosses with *pn2a* and *m100* rearrangements resulting in appearance of conspicuous amounts of the *l74*/R/*Y* females in experiment 1. The cases where nondisjunction interfered with evaluation of variegation are indicated as not tested (nt). In experiment 1 (*r24*) and in all the stocks in experiment 2, *Y* chromosome was substituted to $B^{S}Y$ to discern the females carrying *Y* chromosome. Viability was estimated by percentage of R-carrying females to *FM7*/*l74* sisters. Cases of significant decrease of viability values (χ^2 criterion) are underlined ($P < 0.001$ for all three cases). Two numbers in parentheses indicate: viability, the numbers of R/*l74* (or R/*l74*·Y) and *FM7*/*l74* sisters, respectively; wings with cuts, the numbers of wings with cuts and total numbers of scored wings; wings apart, the numbers of individuals with enlarged angle between wings and total numbers of scored individuals. Total number of scored eyes for "% of eye surface" is indicated in parentheses. No significant differences in viability (*r4*, *r20*, *r24*, and *r9*) as well as frequencies of wings with cuts and wings apart phenotypes (*r9*) were detected between the R/*l74* and R/*l74*·Y females. In other cases of differences between R/*l74* and R/*l74*·Y are highly significant ($P < 0.001$; Fisher's *F* criterion). Fisher's *F* criterion for evaluation percentage of cut wings and wings apart and Student's t_{dif} criterion for mean angle and percentage of eye surface were applied. Numbers of asterisks between adjacent figures in vertical columns designate extent of significance of their differences. * $P < 0.05$. ** $P < 0.01$. *** $P < 0.001$.

[a] Rare hatched images stick to medium before unfolding of wings. The whole eye surface of these individuals shows disturbed faceting (see Figure 5).

[b] Values over 30° and 45° between wings were taken as an indication of mutant phenotype in experiments 1 and 2, respectively.

[c] Mean angle (MA) in degrees was calculated as $MA = (\Sigma A_a + nA_n)N$, where ΣA_a is the sum of abnormal angles (see materials and methods for details); A_n, normal angle; *n*, number of flies with normal angle; *N*, total number of flies scored. Normal angle equals 20–30°; the A_n value is taken as 25°.

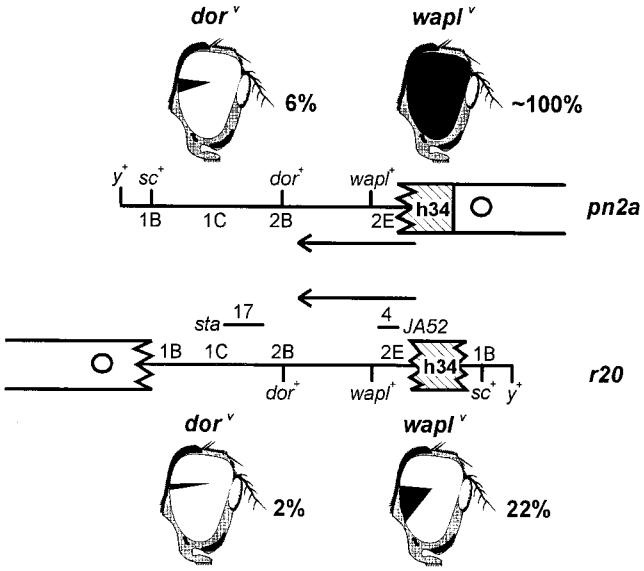

Figure 5.—Patterns of the *dor* (percentage of yellowish eye surface) and *wapl* (percentage of eye surface with disturbed faceting) loci inactivation in *In(1LR)pn2a* (top) and r20 (bottom). The percentages of mutant eye tissue are depicted as blackened sectors. The number of essential loci uncovered by *Df(1)sta* and *Df(1)JA52* is indicated above the bars designating the deficiencies (Lindsley and Zimm 1992). Arrows indicate the direction of inactivation.

may reach *wapl* (2E region) starting from the main heterochromatic block containing the centromere (Figure 5). First, polytene chromosome analysis revealed no heterochromatization of the 1B-2C region juxtaposed to the centromere. Second, *wapl* variegation is stronger than *dor* variegation both in *r20* and in the original *pn2a* rearrangement. The area of irregular facets achieves one-fifth of the eye surface in *r20*/*wapl* females (Table 2), in which *r20* is maternally inherited, whereas barely 2% of eye surface with altered pigmentation is detected in *r20*/*dor* females (Table 3; Figure 5), despite the fact that in this case *r20* is paternally inherited and should therefore exert an enhanced variegation (Spofford 1976). Thus, inactivation in both *r20* and *pn2a* appears to start from region h34, consistently affecting only the expression of the juxtaposed *wapl* gene (Figure 5).

Finally, comparison of the viability of females carrying the *r20* rearrangement over a series of deficiencies uncovering Bridges sections 1 and 2 strongly supports our hypothesis that in *r20* variegation spreads from the small heterochromatic block h34 (Figure 5; Table 4). Deficiency *Df(1)JA52* removes 4 vital loci (Lindsley and Zimm 1992). Inviability of both *r20*/*Df(1)JA52* and *pn2a*/*Df(1)JA52* females indicates a strong inactivation of several vital loci localized distal to the *wapl* gene (Figure 5; Table 4). By contrast, no decrease in viability of *r20*/*Df(1)sta* females was observed, although this deletion is more extended and uncovers at least 17 vital loci (Lindsley and Zimm 1992) that in *r20* are situated closer to the main heterochromatic block than the *dor* locus (Figure 5). Thus, we have compelling evidence that in *r20 wapl* inactivation starts from the h34 block. The inability of comparably small (*r30*) or even larger acentric heterochromatic blocks (*r35*) to induce PEV might depend on their distance from the bulk of *X* heterochromatin and thus their distance from the chromocenter (see discussion).

DISCUSSION

In contrast with the advanced understanding of *trans*-acting factors, little is known of *cis*-acting requirements for PEV. Here we have addressed this problem by dissecting a heterochromatic block capable of inducing PEV. In the *In(1LR)pn2a* rearrangement virtually the whole *X*-linked heterochromatin is moved adjacent to the euchromatic region 2E, causing inactivation of genes located up to ~600 kb from the breakpoint region (Tolchkov *et al.* 1984, 1997). We used an efficient genetic system to recover partial or full PEV revertants represented by secondary rearrangements. This approach allowed us to correlate the size and the internal structure of different portions of *Xh* with the strength

TABLE 3

Inactivation of the *dor* locus in *pn2a* and *r20* rearrangements

	Eyes with yellowish spots (%), dor^V		% of yellowish eye surface	
Experiments	*pn2a*/*dor*^{1}	*r20*/*dor*^{1}	*pn2a*/*dor*^{1}	*r20*/*dor*^{1}
1	38.1 (45/118)	20.1 (27/134)	5.2 ± 1.1	2.8 ± 0.7
2	43.2 (57/132)	13.6 (16/118)	5.8 ± 1.2	1.4 ± 0.6
Total	40.8 (102/250)	17.1 (43/252)	5.5 ± 0.8	2.1 ± 0.4

dor inactivation was tested in the R/*dor*^{1} females (progeny of *dor*^{1}/*FM7* females crossed to R/*Y* males), where R designates *pn2a* or *r20* rearrangement. Values in parentheses indicate the number of eyes with yellowish spots and the number of scored eyes, respectively. Differences in "eyes with yellowish spots" between *pn2a* and *r20* rearrangements are significant in both experiments ($P < 0.01$ for experiment 1 and $P < 0.001$ for experiment 2 and total using Fisher's *F* criterion). Differences in "% of yellowish eye surface" between *pn2a* and *r20* rearrangements are significant in experiment 2 ($P < 0.01$) and total data ($P < 0.001$) according to Student's t_{dif} criterion.

TABLE 4

Viabilities of females carrying *pn2a* or *r20* rearrangements (R) and deficiencies uncovering regions of putative inactivation

	Paternally inherited R		Maternally inherited R	
Df(1)	*pn2a*/*Df(1)*	*r20*/*Df(1)*	*pn2a*/*Df(1)*	*r20*/*Df(1)*
JA52	0 (0/326)	(2/596)	nt	nt
sta	115 (299/260)	103 (349/338)	104 (619/594)	105 (351/334)

Viability of R/*Df(1)JA52* females was estimated as the ratio of *TM2*/+ females to *Dp(1;3)w*^{vco}/+ females, produced in cross [♀♀*Df(1)*/*Df(1);Dp(1;3)w*^{vco}/*TM2* × ♂♂R/*Y*]. Viability of R/*Df(1)sta* females was estimated in crosses [R/*FM7* × *Df(1)sta*/*Dp.Y*] or [*Df(1)sta*/*FM7* × R/*Y*] as the ratio of R/*Df(1)sta* to *FM7*/*Df(1)sta* females or R/*Df(1)sta* to R/*FM7* females, respectively. In these cases effects of maternal or paternal inheritance of a rearrangement were evaluated. Two numbers in parentheses indicate the number of female R/*Df(1)sta* and sisters carrying *FM7* [or R/*Df*(1)*JA*52; TM2/+ and sisters carrying *Dp(1;3) w*^{vco}], respectively.

of PEV affecting the *wapl* gene, spaced ~50 kb from the eu-heterochromatin boundary.

The strength of PEV positively correlates with the size of the *cis*-acting heterochromatic blocks: We characterized PEV strength by both the wing phenotypes and the relative size of mutant eye surface. PEV strength was shown to decrease with the size of the adjacent centromere containing heterochromatic block in rearrangements *pn2a*, *m141*, *r4*, *m100*, and *r24* (Table 2; Figure 6). These results suggest that the whole *X*-linked heterochromatic block, including nine cytologically defined segments (Gatti and Pimpinelli 1992; Gatti *et al.* 1994), is involved in PEV induction. Removal of the distal h26 section of heterochromatin in the *m141* rearrangement is enough to produce a marked decrease of variegation (Table 2). Thus, a relatively small *Xh* region, placed at ~15–20 Mb from the eu-heterochromatic boundary, appears to play a significant role in the inactivation of euchromatic genes. Removal of *Xh* segments containing the NO (*r4*), the 1.688 complex satellite (*m100*), and virtually the entire heterochromatic material of the left arm (*r24*) resulted in further and gradual weakening of inactivation (Figure 6).

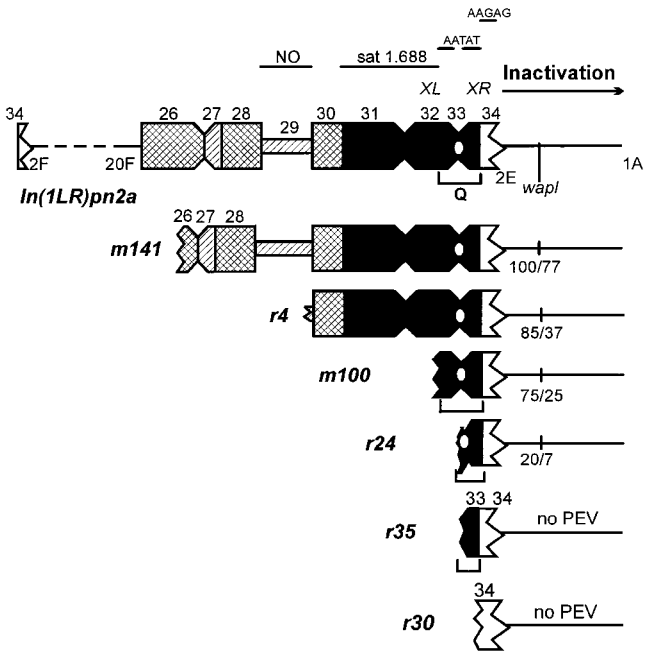

Figure 6.—Correlation between decrease of *wapl* gene inactivation and reduction of the *cis*-acting heterochromatic block. The arrangement of NO, complex satellite 1.688, and AATAT and AAGAG simple satellite sequences is shown. The numbers separated by slashes indicate the percentage of "wing with cuts" and "disturbed eye faceting areas," respectively. Segments h34 and h33 are disproportionally enlarged.

Evidence of a positive correlation between the size and the PEV-inducing potential of a given heterochromatic block had been reported previously for the derivatives of a rearrangement transposing the *white* gene to the heterochromatin of chromosome *4* (Panshin 1938). The diminishing of heterochromatic masses adjacent to the *white* locus was indirectly estimated judging by the extent of coupled variegation of chromosome *4* heterochromatic *ci* gene. More recently, however, the strength of *white* variegation was shown to be independent of the amount of adjacent *2h* material (Howe *et al.* 1995). The apparent contradiction between this and our results might be explained by taking into account that in the experiments by Howe and co-workers variegation was estimated in rearrangements with different euheterochromatic junctions, whereas in our rearrangements this junction is unchanged. Dorer and Henikoff (1997) presented a similar conclusion in their studies of *cis*-silencing effects caused by transgene arrays. These arrays are considered as heterochromatic insertions and the degree of silencing was shown to be dependent on the size of arrays.

The observed conspicuous contribution to PEV of the small distal h26 fragment, comprising a negligible amount (~5%) of the genomic heterochromatin, suggests that *X* heterochromatin may act as an autonomous unit, relatively independent of the rest of heterochromatin. Interestingly, recent fluorescent *in situ* hybridization (FISH) analysis of the arrangement of heterochromatic components within interphase nuclei indicates that

each chromosome has its own "heterochromatic compartment" in the Drosophila genome (Dernburg *et al.* 1996).

Taking into account that dominant *trans*-acting modifiers of PEV are not known on the *X* chromosome, one may suppose that some of the observed effects might be attributed to the action of dominant *trans*-acting suppressors induced by irradiation in autosomes. However, the following arguments favor decreased *cis*-action of truncated heterochromatic blocks.

First, the observed conspicuous correlation between the size of the adjacent heterochromatic block and the degree of silencing of the *wapl* gene is difficult to explain by the action of *trans*-modifiers. Second, no rearrangements without *X* chromosome heterochromatin breakage were detected among the 22 selected reversions. The cases of full reversion of PEV (*r16* and *r35*) can hardly be attributed to the effect of a putative extremely strong autosomal suppressor, since the tested strong autosomal suppressors [*Su-var(3)9* and others] cause only negligible effects, resulting in no more than a 10% decrease of the number of cut wings in *pn2a* and *r24*, as compared to the drastic influence of the heterochromatic *Y* chromosome resulting in full reversion of PEV in *r24*.

Removal or distancing of the centromere region from the eu-heterochromatic boundary results in reversion or attenuation of PEV: PEV was not detected in *r30* (Tolchkov *et al.* 1997) and *r35* rearrangements (Figure 6) where the 2E polytene region is situated near *XR* material lacking the centromere. This result could depend on the sensitivity of our genetic test, which might be inadequate to detect drastically weakened PEV induced by small heterochromatin masses. However, PEV was observed in *r24*, a rearrangement bearing a comparably small, but centromere-containing, heterochromatic block near 2E. The following indirect observations also suggest a crucial role of centromere in inactivation. The size of the heterochromatic block near 2E is not changed in *r9*, but the rearrangement results in spacing of the centromere from the eu-heterochromatic junction (Figure 7) and is associated with negligible *wapl* variegation. No PEV was detected in *r16*, where a conspicuous heterochromatic block lacking the centromere remains in the vicinity of 2E (Figure 7). Thus, the preservation of a significant mass of the *Xh* block may be insufficient to induce PEV on the adjacent euchromatic genes, if it lacks the centromere. The disappearance of PEV in *r16* and its drastic weakening in *r9* may be caused either by peculiar properties of the heterochromatic blocks fused to the h34 segment or by a disruption of the continuity of the heterochromatic region encompassing h34 and the centromere (see below).

If the centromere (h33 region) is the inactivation center, it is likely that its separation from the 2E euchromatin would result in complete reversion of inactivation. However, the absence of strong inactivation of the eu-

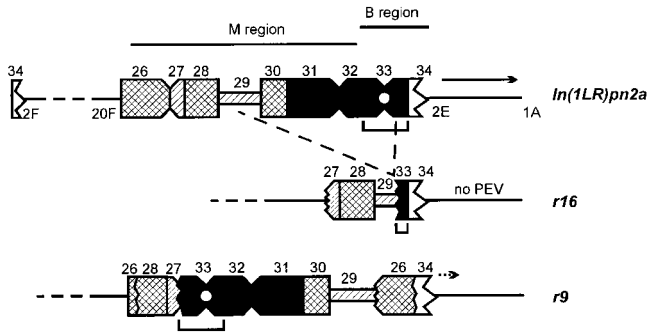

Figure 7.—PEV and structures of rearrangements *pn2a*, *r9*, and *r16*. Arrow lengths arbitrarily indicate the strength of PEV exerted by rearrangements. The sizes of the putative basic (B) and modulating (M) regions are indicated.

chromatic genes localized near the centromeric heterochromatin in *r20* (Figure 5; Table 4) contradicts this hypothesis. Alternatively, inactivation may be exerted via the concerted action of the h34 segment and the centromere region. Separation of the components of this putative integral block may result in the reversion of PEV observed in *r30* and *r35* (Figure 6). Actually, substitution of the centromere-associated region with other *Xh* segments (*r16*) fails to restore inactivation (Figure 7) and spacing of the centromere region from the eu-heterochromatic junction results in similar effects (*r9*).

We suppose that the centromere affects by distance-dependent interactions the state of at least some segments of the heterochromatic block harboring it. The published data show that the above hypothesis may be true for other models as well as for our model. Centromere separation resulted in variegation of the heterochromatic *peach* gene in *Drosophila virilis*, although the bulk of heterochromatin remains attached to the *peach* gene in the $T(3;5)pe^{m5}$ rearrangement (Baker 1954). The participation of the centromere in the maintenance of the *light (lt)* gene activity can be deduced by the localization of the breakpoints inducing *lt* variegation. Actually, variegation of *lt*, localized in the distal 2L heterochromatin, is observed as a result of proximal breakages in 2L heterochromatin, just distal to the centromere (Lohe *et al.* 1993), whereas no *lt* variegation was detected as a result of 2R heterochromatin separation from the centromere.

The lack of full reversion of *white* variegation in a $T(1;4)w^{m11}$ derivative resulting in centromeric region detachment (Panshin 1938) indicates that the effect of the centromere on PEV intensity may vary in different rearrangements. The nature and size of the heterochromatic block, the localization of the centromere inside this block, and the distance between the breakpoint and the reporter gene may modulate centromere effects.

PEV in *r20* and association of heterochromatic blocks: The strong PEV observed in *r20* is intriguing, since an

acentric piece of *XR* in all the other rearrangements of class 3 is incapable of causing variegation of the adjacent 2E region. The sizes of blocks carrying the h34 segment in *r20* and in *r30* are comparable, while the size of the h33d Q-bright segment adjacent to 2E is even larger in *r35* than in *r20* (Figure 3). On the other hand, the distance of the eu-heterochromatic boundary from the pericentric heterochromatin amounts to 8 or more sections of the Bridges map in *r30*, *r35*, and other rearrangements of class 3, and only to 1.5 sections in *r20*. We suppose that in *r20* a contact between the small acentric block and the chromocenter can occur, which in the other rearrangements of this class is impaired by the distance of the acentric *XR* block from the centromeric region. Actually, close pairing of the h34 region with the chromocenter was consistently detected in 100% of salivary gland nuclei bearing the *r20* chromosome, where the 1B-2E polytene region looks like a loop associated with the chromocenter. Other rearrangements of this class (*r30* and *r35*) in heterozygotes with structurally normal chromosomes show no notable association of the separated heterochromatic blocks with the chromocenter (~40 nuclei were analyzed for each rearrangement). This pairing would be the basis of the PEV-inducing capability observed in *r20*. These observations are in agreement with previous data indicating that PEV strength depends on the distance between variegating breakpoints and pericentromeric heterochromatin (Wakimoto and Hearn 1990; Eberl *et al.* 1993; Konev 1994, 1995; Talbert *et al.* 1994; Henikoff *et al.* 1995; Csink and Henikoff 1996).

The *r20*, *r30*, and *r35* rearrangements carry near the 2E region the h34 block, containing the AAGAG satellite (Lohe *et al.* 1993; Tolchkov *et al.* 1997). The block of AAGAG satellite of comparable size (Csink and Henikoff 1996; Dernburg *et al.* 1996) inserted into the *bw* gene (bw^D) causes *trans*-inactivation of bw^+ in bw^D/bw^+ heterozygotes, but no *cis*-inactivation of neighboring genes (Talbert *et al.* 1994). However, bw^D insertion starts to cause *cis*-inactivation if the distance between the insertion and the chromocenter is shortened (Talbert *et al.* 1994). Thus, h34 block and bw^{+D} insertion are similar in their ability to cause *cis*-inactivation.

The strong effect of a small heterochromatic segment on PEV: A comparison of the variegation strength in *r4*, *m100*, and *r24* rearrangements reveals the crucial role of a restricted block of pericentric *Xh* in inducing PEV. The difference in PEV severity between *m100* and *r4* is modest, consisting only in a decreased amount of mutant eye surface in *m100*, with other traits showing no significant differences of variegation (Table 2; Figure 6). The size of the *cis*-acting *Xh* block is much smaller in *m100* than in *r4*; *m100* lacks segments h30-h32, encompassing ~11 Mb of the *X*-specific complex 1.688 satellite (Lohe *et al.* 1993; Pimpinelli *et al.* 1995). On the other hand, a slight decrease of the *cis*-acting *Xh* block in *r24* results in a significant decrease of PEV (Figure 6). Roughly estimating, half of the Q-bright material is removed in *r24* as compared to *m100* (Figure 3). It is assumed that Q-bright regions mainly contain AATAT satellite sequences (Lohe *et al.* 1993). Taking into account the calculated amount of this satellite within *Xh* (0.4–0.6 Mb; Lohe *et al.* 1993; Sun *et al.* 1997), *cis*-acting *Xh* regions in *m100* and *r24* should differ for ~0.2–0.3 Mb of AATAT satellite. Thus, the 0.3-Mb segment of AATAT satellite present in *m100* seems to contribute to PEV much more than the 11-Mb block of complex satellite present in *r4*.

The amount of Q-bright material is comparable in both the centric *r24* and acentric *r35* heterochromatic fragments (Figure 3), but only *r24* exerts a significant PEV on the adjacent euchromatic genes, thus suggesting that a functional centromere plays a central role in inducing variegation.

Interactions of the *Xh* segments contribute to PEV: On the basis of the obtained results, we propose a model in which the pericentric region encompassing AATAT (h33) and AAGAG (h34) satellites can be referred to as basic region (B region), indispensable in causing strong PEV (Figure 7). The distal part of *Xh* can be considered as a modulating element (M region), capable of significantly enhancing PEV. Disruption of the B region can lead to full reversion (*r30*, *r35*, and *r16*), strong suppression (*r9*), or substantial decrease of PEV even in the presence of an insignificant decrease of the *cis*-acting heterochromatic mass (*r24*). We suppose that putative components of a disrupted B region may cause PEV if they are sufficiently close to each other to be able to associate. This could explain why *r20*, which carries moderately spaced pieces of the interrupted B region (h34 and h33), can induce strong variegation (Figure 5), while *r9*, in which the B-region components are more widely spaced and thus almost incapable of associating with each other, can induce only weak PEV. In other words, the spatial interaction of the B-region "modules," rather than its integrity, seems to be important for the induction of strong PEV. We propose that the centromere *per se* and simple satellite sequences contained in the B region can interact to form a spatial complex with a definite interior architecture that is indispensable in inducing strong PEV. Chromatin conformation in this "inactivation complex" would be dramatically changed, so that the inactivation potential of the complex largely exceeds the additive potentials of its components. The same sequences, once excluded from the inactivation complex, could exert only a weak influence on the neighboring euchromatic genes. If the B-region modules are able to form the putative inactivation complex, then the M-region material can affect it by enhancing its inactivation potential, probably by attracting proteins common to the M and B regions.

Howe *et al.* (1995) showed that small reduction of the heterochromatic block size at the expense of euchromatin-adjacent sequences caused drastic changes

in *w* variegation severity. The variegation strength in this case does not correlate with the size of the heterochromatic block. On the basis of the results the authors concluded "that the severity of variegation of the euchromatic *w* gene was not indicative of the quantity of adjacent heterochromatin . . . rather *w* variegation was sensitive to the nature of the juxtaposed repetitive DNA" (Weiler and Wakimoto 1998). This conclusion is in accordance with our concept; a relatively small heterochromatic segment adjacent to euchromatin (B region) exerts a crucial effect on the intensity of PEV induced by the large heterochromatic block.

A B-like complex could also be formed in autosomal heterochromatin (*Ah*). This assumption might explain the differences of bw^D interactions with *Xh* and *Ah* (Talbert *et al.* 1994; Henikoff *et al.* 1995). In the case of the bw^D translocations to the *X* chromosome proximal euchromatin the huge M region lacking simple satellites may impede the interaction of the bw^D insertion with B region. In this case bw^D variegation is suppressed (Talbert *et al.* 1994). By contrast, *Ah* with centrally located centromere and dispersed simple satellites segments (Lohe *et al.* 1993) may provide more suitable conditions for such interactions.

Our results imply that strong PEV can be induced as a result of specific interactions between various heterochromatic repeats, whereas sometimes variegation is known to be induced solely due to the presence of a definite number of identical repeated sequences (Dorer and Henikoff 1994). We propose the existence of two types of interaction between heterochromatin segments: specific interactions mediated by the centromere region and simple satellites as well as less specific interactions responsible for the effect of the size of *cis*-acting heterochromatin (M-B interactions in our terms). The centromere probably affects the state of the whole heterochromatic block or at least some of its segments.

We thank G. L. Kogan and S. A. Lavrov for providing advice and unpublished results. We thank V. E. Alatortsev, S. G. Balashova, B. O. Glotov, A. B. Devin, E. G. Pasyukova, J. M. Rozovsky, and Y. Y. Shevelev for their relevant comments and suggestions. We thank S. A. Lavrov for his help in preparing figures. We also thank two anonymous reviewers whose comments considerably improved this manuscript. This research was supported by grants from the Russian Foundation of Basic Researches (99-04-48561 and 96-15-98072) and the Russian Program "Frontiers in Genetics" (99-1-069) to V.A.G.

LITERATURE CITED

Alatortsev, V. E., E. V. Tolchkov, S. Y. Slobodyanyuk and V. A. Gvozdev, 1982 Cellular variegation and antigen disappearance as a result of the position effect of the *Pgd* locus in *Drosophila melanogaster*. Genetika (Russ.) **18:** 13–23.

Alatortsev, V. E., I. A. Kramerova, M. V. Frolov, S. A. Lavrov and E. D. Westphal, 1997 *Vinculin* gene is non-essential in *Drosophila melanogaster*. FEBS Lett. **413:** 197–201.

Baker, W. K., 1954 The anatomy of the heterochromatin. Data on the physical distance between breakage point and the affected locus in V-type position effect. J. Hered. **45:** 65–68.

Csink, A. K., and S. Henikoff, 1996 Genetic modification of heterochromatic association and nuclear organization in Drosophila. Nature **381:** 529–531.

Dernburg, A. F., K. W. Broman, J. C. Feng, W. F. Marshall, J. Philips *et al.*, 1996 Perturbation of nuclear architecture by long-distance chromosome interaction. Cell **85:** 745–759.

Dorer, D. R., and S. Henikoff, 1994 Expansions of transgene repeats cause heterochromatin formation and gene silencing in Drosophila. Cell **77:** 993–1002.

Dorer, D. R., and S. Henikoff, 1997 Transgene repeat arrays interact with distant heterochromatin and cause silencing in *cis* and *trans*. Genetics **147:** 1181–1190.

Eberl, D. F., B. J. Duyf and A. J. Hilliker, 1993 The role of heterochromatin in the expression of a heterochromatic gene, the rolled locus of *Drosophila melanogaster*. Genetics **134:** 277–292.

Gatti, M., and S. Pimpinelli, 1992 Functional elements in *D. melanogaster* heterochromatin. Annu. Rev. Genet. **26:** 239–275.

Gatti, M., S. Bonaccorsi and S. Pimpinelli, 1994 Looking for Drosophila mitotic chromosomes. Methods Cell Biol. **44:** 371–391.

Grigliatte, T., 1991 Position effect variegation: an essay for nonhistone chromosomal proteins and chromatin assembly and modifying factors, pp. 587–627 in *Functional Organization of the Nucleus: A Laboratory Guide*, edited by B. A. Hamkali and S. C. R. Elgin. Academic Press, San Diego.

Gvozdev, V. A., S. A. Gostimsky, T. I. Gerasimova, E. S. Dubrovskaya and O. Y. Braslavskaya, 1975 Fine genetic structure of the 2D3-2F5 region of the X chromosome of *D. melanogaster*. Mol. Gen. Genet. **141:** 269–275.

Henikoff, S., 1990 Position effect variegation after 60 years. Trends Genet. **6:** 422–426.

Henikoff, S., 1997 Nuclear organizations and gene expression: homologous pairing and long range interactions. Curr. Opin. Cell Biol. **9:** 388–395.

Henikoff, S., J. M. Jackson and P. B. Talbert, 1995 Distance and pairing effects on the $brown^{Dominant}$ heterochromatic elements in Drosophila. Genetics **140:** 1007–1017.

Hilliker, A. J., and C. B. Sharp, 1988 New perspectives on the genetic and molecular biology of constitutive heterochromatin, pp. 91–115 in *Chromosome Structure and Function*, edited by J. P. Gustafson, R. Appels and R. Kaufman. Plenum, New York.

Howe, M., P. Dimitri, M. Berloco and B. T. Wakimoto, 1995 *Cis*-effects of heterochromatin on heterochromatic and euchromatic gene activity in *D. melanogaster*. Genetics **140:** 1033–1045.

Ilyina, O. V., A. V. Sorokin, E. S. Belyaeva and I. F. Zhimulev, 1980 New mutants. Dros. Inf. Serv. **55:** 205.

Jenuwein, T., G. Laible, R. Dorn and G. Reuter, 1998 SET domain proteins modulate chromatin domains in eu- and heterochromatin. Cell. Mol. Life Sci. **54:** 80–93.

Konev, A. Y., 1994 Proximity dependent interaction between heterochromatic regions may be important for euchromatic loci position effect variegation. 35th Annual Drosophila Research Conference, Chicago. 325B.

Konev, A. Y., 1995 Cytogenetical study of 44F-45D region of chromosome 2 in *D. melanogaster*. Ph.D. Thesis, Sanct-Petersburgh. (Russian).

Lindsley, D. L., and G. G. Zimm, 1992 *The Genome of D. melanogaster*. Academic Press, San Diego.

Lohe, A. R., and A. J. Hilliker, 1995 Return of the H-word (heterochromatin). Curr. Opin. Genet. Dev. **5:** 746–755.

Lohe, A. R., A. J. Hilliker and P. A. Roberts, 1993 Mapping simple repeated DNA sequences in heterochromatin of *D. melanogaster*. Genetics **134:** 1149–1174.

Makunin, I. V., G. V. Pokholkova, S. O. Zakharkin, N. G. Kholodilov and I. F. Zhimulev, 1995 Isolation and characterization of the repeated DNA sequences from the centric heterochromatin of the second chromosome of *D. melanogaster*. Dokl. Akad. Nauk (Russ.) **344:** 266–269.

McKee, B. D., 1996 The licence to pair: identification of meiotic pairing sites in Drosophila. Chromosoma **105:** 135–141.

Panshin, I. B., 1938 The cytogenetic nature of the position effect of the genes *white* (*mottled*) and *cubitus interruptus*. Biologicheskij Z. **7:** 837–868.

Pimpinelli, S., M. Berloco, L. Fanti, P. Dmitri, S. Bonaccorsi *et al.*, 1995 Transposable elements are stable structural compo-

nents of *Drosophila melanogaster* heterochromatin. Proc. Natl. Acad. Sci. USA **92:** 3804–3808.

Pokholkova, G. V., I. V. Makunin, E. S. Belyaeva and I. F. Zhimulev, 1993 Observation on the induction of position effect variegation of euchromatic genes in *D. melanogaster*. Genetics **134:** 231–242.

Reuter, G., and P. Spierer, 1992 Position effect variegation of euchromatic genes in *D. melanogaster*. Bioessays **14:** 605–612.

Spofford, J. B., 1976 Position effect variegation in Drosophila, pp. 955–1019 in *Genetics and Biology of Drosophila*, edited by M. Ashburner and E. Vovitski. Academic Press, London.

Sun, X., J. Wahlstrom and G. Karpen, 1997 Molecular structure of a functional Drosophila centromere. Cell **91:** 1007–1019.

Talbert, P. B., C. D. S. Leciel and S. Henikoff, 1994 Modification of the Drosophila heterochromatic mutation *brown*^{Dominant} by linkage alteration. Genetics **136:** 559–571.

Tartof, K. D., C. Hobbs and M. Jones, 1984 A structural basis for variegation position effects. Cell **37:** 869–878.

Tolchkov, E. V., M. D. Balakireva and V. E. Alatortsev, 1984 Inactivation of the X chromosome region with a known fine genetic structure as a result of the variegated position effect in *D. melanogaster*. Genetika (Russ.) **20:** 1846–1856.

Tolchkov, E. V., I. A. Kramerova, S. A. Lavrov, V. I. Rasheva, S. Bonaccorsi *et al.*, 1997 Variegated position effect in *D. melanogaster* X chromosome inversions with a breakpoint in satellite block. Chromosoma **106:** 520–525.

Wakimoto, B. T., and M. G. Hearn, 1990 The effect of chromosome rearrangements on the expression of heterochromatic genes in chromosome *2L* of *D. melanogaster*. Genetics **125:** 141–154.

Weiler, K. S., and B. T. Wakimoto, 1995 Heterochromatin and gene expression in Drosophila. Annu. Rev. Genet. **29:** 577–605.

Weiler, K. S., and B. T. Wakimoto, 1998 Chromosome rearrangements induce both variegated and reduced, uniform expression of heterochromatic genes in a development-specific manner. Genetics **149:** 1451–1464.

Zhimulev, I. F., 1998 Polytene chromosomes, heterochromatin and position effect variegation. Adv. Genet. **37:** 1–566.

Communicating editor: S. Henikoff